

Operation features of a longitudinal-capacitive-discharge-pumped CuBr laser

F.A. Gubarev, V.B. Sukhanov, G.S. Evtushenko, D.V. Shiyarov

Abstract. The frequency and energy characteristics of a capacitive-discharge-pumped CuBr laser are investigated. Processes proceeding in the discharge circuit of lasers pumped in this way, in particular, pumped without an external storage capacitor are analysed. It is shown that, depending on the pumping circuit, laser levels are excited either during the charge current flow or during the discharge of electrode capacitances. The differences in the influence of the active HBr addition on the characteristics of the discharge and lasing compared to the case of a usual repetitively pulsed high-current discharge with internal electrodes are established.

Keywords: copper bromide laser, capacitive discharge, excitation, modified kinetics, active additions.

1. Introduction

A search for new methods of pumping active media, in particular, new pumping circuits, is a promising direction in the study of metal vapour lasers. Self-contained metal vapour lasers are usually pumped by a high-current glow discharge with electrodes placed inside a gas-discharge tube (GDT) [1, 2]. Metal ion vapour lasers are also pumped by a transverse capacitive discharge with external electrodes [3, 4]. The use of capacitive discharges considerably simplifies a GDT design and excludes a direct contact of electrodes with gas. The latter can be useful when active media contain chemically aggressive substances. In particular, the use of barrier and capacitive discharges provided a substantial increase in the service life of excilamps [5]. The advantages of using the capacitive discharge for pumping CuBr–HBr lasers are pointed out in paper [6], where the

development of a self-contained metal vapour laser pumped by a longitudinal capacitive discharge was reported.

The aim of the present paper is to study the frequency and energy characteristics of capacitive-discharge-pumped CuBr lasers, in particular, with HBr additions, the achievement of practically significant output powers and lasing efficiencies, and also to investigate processes in the discharge circuit of the laser and features of the capacitive-discharge pumping of metal halide vapour lasers with the help of probes placed in the electrode regions of the GDT.

2. Experimental

Figure 1 shows the scheme of the experimental setup for studying the energy characteristics of capacitive-discharge-pumped CuBr lasers. No probes were used in the study. The GDT wall in the electrode region is shown by a double straight line. Two quartz GDTs with a discharge channel of length 38 cm and internal diameters 1.0 and 2.7 cm were used. The electrodes made of a tantalum foil had a width of 10 cm and diameter of 5 cm. They were placed on the external wall of the tube at a distance of 44 cm from each other. Because the electric coupling of a plasma with electrodes located on the external wall is capacitive and the distance between electrodes considerably exceeds the electrode width, we call such a discharge a longitudinal capacitive discharge. Unlike the design used in [6], the tube diameter in the electrode region was greater than the discharge channel diameter, which provided an increase in the energy supply to the discharge. We used three pumping

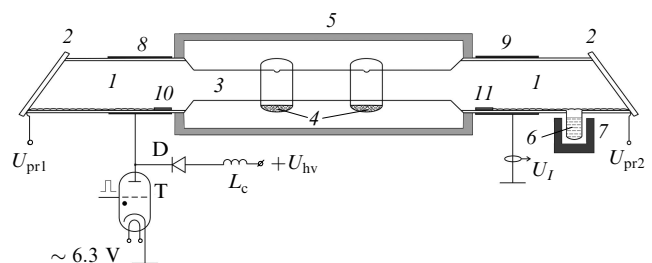


Figure 1. Scheme of the experiment: (1) GDT electrode region; (2) windows; (3) discharge channel; (4) copper bromide powder; (5) external heater; (6) HBr generator; (7) heater; (8, 9) cylindrical electrodes; (10, 11) metal plates (probes); (T) tacitron; (L_c and D) charging choke and diode, respectively (circuit without the external storage capacitor); (U_1) current sensor signal; (U_{pr1} and U_{pr2}) probe voltages; (U_{hv}) output voltage of a high-voltage rectifier.

F.A. Gubarev V.E. Zuev Institute of Atmospheric Optics, Siberian Branch, Russian Academy of Sciences, pl. Akad. Zueva 1, 634021 Tomsk, Russia; Tomsk Polytechnic University, prosp. Lenina 30, 634050 Tomsk, Russia;

G.S. Evtushenko Tomsk Polytechnic University, prosp. Lenina 30, 634050 Tomsk, Russia; e-mail: ime@tpu.ru;

V.B. Sukhanov, D.V. Shiyarov V.E. Zuev Institute of Atmospheric Optics, Siberian Branch, Russian Academy of Sciences, pl. Akad. Zueva 1, 634021 Tomsk, Russia

Received 17 December 2008; revision received 21 August 2009

Kvantovaya Elektronika 40 (1) 19–24 (2010)

Translated by M.N. Sapozhnikov

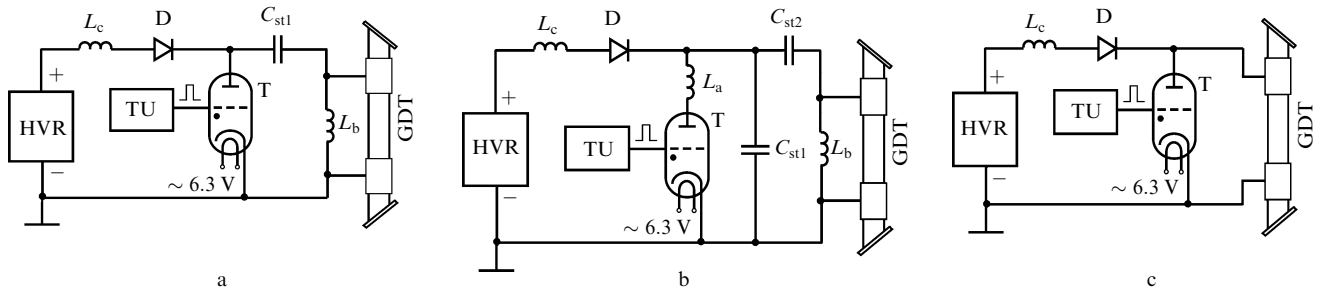


Figure 2. Pumping circuits: circuit of the directly discharged storage capacitor (direct circuit) (a), Blumlein voltage-doubling circuit (b), and circuit without the external storage capacitor (c); (HVR) high-voltage rectifier; (TU) triggering unit; (L_c and D) charging choke and diode, respectively; (C_{st1} and C_{st2}) storage capacitors; (L_b) shunting inductance; (L_a) auxiliary choke; (T) TGU1-1000/25 tacitron.

circuits: the circuit of a direct discharge of a storage capacitor (Fig. 2a), the Blumlein voltage-doubling circuit (Fig. 2b), and the circuit without an external storage capacitor (Fig. 2c). The latter circuit does not contain a storage capacitor and a shunting inductance, and the GDT self-capacity (the equivalent electrode capacity) plays the role of the energy storage system. This simplifies the pumping circuit and allows one to exclude a circuit formed by a shunting inductance and the GDT from the discharge circuit of the laser. The optimal capacities of storage capacitors C_1 and C_2 were selected experimentally to provide the maximum average lasing power. They were $C_1 = 110$ pF for the direct discharge circuit of the storage capacitor and $C_1 = 110$ pF and $C_2 = 235$ pF for the Blumlein voltage-doubling circuit. Because of a low optimal working capacity when the capacitive discharge was used, the energy losses in the pumping circuit can reduce the lasing efficiency to a greater extent than in the conventional circuit. This is especially important at high pulse repetition rates, when energy losses in a switch (TGU1-1000/25 tacitron) increase [7].

The required temperature of the discharge channel was maintained by heating externally the GDT active region. The temperature regime of the GDT of the design used here, in particular, the temperature of containers with copper bromide and the temperature profile inside the GDT are determined both by the external heating energy and the energy released in the discharge, which depends on the pumping circuit efficiency. Therefore, the optimal temperature of a heater was different for different circuits and was in the range from 720 to 770 K. The optimal pressure of the buffer neon gas, at which experiments were performed, was 30 Torr. The average lasing power changed insignificantly in the buffer gas pressure range from 10 to 30 Torr. The output power began to decrease considerably at pressures above 30 Torr. The HBr molecules were introduced with the help of a reverse HBr generator [8]. The HBr pressure was controlled by the heater temperature within 0.1–0.3 Torr and its optimal value was determined by the maximum of the output power.

The voltage, current and laser pulses were recorded with a Tektronix P6015A voltage probe, a Pearson Current Monitor 8450, and a FK-22 coaxial photocell, respectively. The average radiation power was measured with an Ophir 20C-SH power meter. The output signals of the power meter were fed to a LeCroy WJ-324 four-channel digital oscilloscope. The oscilloscope was synchronised by the current through the GDT, which begins to flow at the moment of the tacitron switching on. The rest of the oscillograms were

recorded with respect to the current oscillogram. The zero time in figures presented below corresponds to the beginning of the oscilloscope sweep, which was set to achieve the highest information content of recorded oscillograms.

3. Power characteristics of capacitive-discharge-pumped CuBr lasers

A specific feature of the CuBr laser compared to usual copper vapour lasers is the possibility of operating at high pulse repetition rates, both optimal and maximal [9, 10]. The addition of active impurities, in particular, the H_2 and HBr molecules expands the range of pulse repetition rates. The pulse repetition rate can be increased by reducing the energy supplied to the discharge, which assumes in the case of conventional pumping circuits the reduction of the capacity of a storage capacitor. Upon pumping by a capacitive discharge, the energy input to the discharge is limited by the values of barrier capacities, which are $\sim 100 - 200$ pF for GDTs used in the present paper, i.e. the low-energy input regime takes place. Thus, prerequisites exist for obtaining rather high output powers and lasing efficiencies in capacitive-discharge-pumped CuBr lasers at high pulse repetition rates, especially upon the introduction of active additions.

Figure 3 presents the dependences of the average lasing power P_{av} (total at wavelengths 510.6 and 578.2 nm) on the pulse repetition rate f for a CuBr laser with the addition of HBr for different pumping circuits. One can see that capacitive-discharge-pumped CuBr–HBr lasers have the range of pulse repetition rates similar to that of conven-

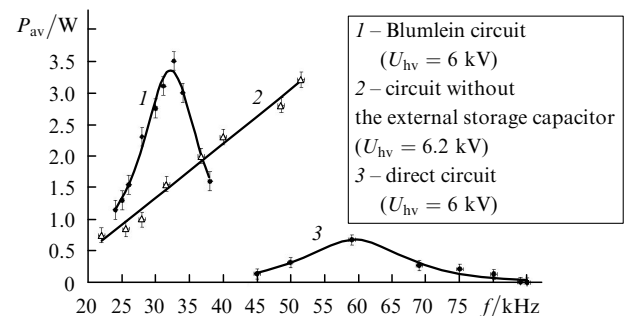


Figure 3. Dependences of the average output power of the CuBr–HBr laser on the pulse repetition rate for different pumping circuits for a GDT of diameter 2.7 cm; U_{hv} is the output voltage of a high-voltage rectifier.

tionally pumped CuBr–H₂(HBr) lasers [11]. Among the pumping circuits considered here, the circuit without the external storage capacitor gives the best result in this respect. After optimisation of pumping conditions by the CuBr and HBr vapour pressures for the given pumping circuits and GDT, we obtained the higher average lasing powers (Fig. 4) than those presented in Fig. 3.

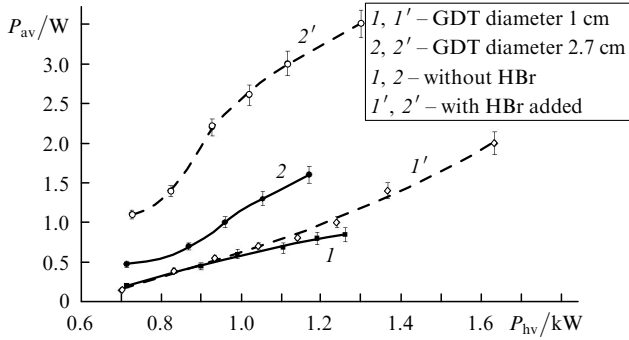


Figure 4. Dependences of the average lasing power on the power consumed from a high-voltage rectifier. Pumping circuit without the external storage capacitor; $f = 37$ kHz, $p_{\text{Ne}} = 30$ Torr.

Table 1 presents the average output powers and efficiencies achieved by using different pumping circuits. The lasing efficiency was calculated by the power consumed from a high-voltage rectifier. The maximum average lasing power of 3.7 W for the efficiency of 0.27 % was obtained in a GDT of diameter 2.7 cm with the addition of HBr by using the Blumlein doubling circuit (1.25 W without the HBr addition). In a GDT of diameter 1.0 cm, the maximum average lasing power was 2 W. Thus, the proposed pumping circuit without an external storage capacitor are not inferior in efficiency than the traditional circuits used for pumping metal vapour lasers. At the same time, this circuit is simpler and, in our opinion, preferable because it contains one pumping circuit (by neglecting parasitic parameters).

It was pointed out in [12] that the addition of small amounts of HBr in the active elements of conventionally pumped CuBr lasers was similar to the addition of hydrogen and considerably improved the lasing parameters. The influence of additions into active elements of a small volume was especially noticeable (the output power increased approximately by a factor of five), whereas the influence of additions into active elements of a larger volume (GDTs

Table 1. Characteristics of capacitive-discharge-pumped CuBr lasers.

GDT diameter/cm	Pumping circuit	HBr presence	Pulse repetition rate/kHz	P_g/W	Efficiency (%)
2.7	direct	absent	57	1.1	0.09
2.7	direct	present	57	0.68	0.06
2.7	Blumlein	absent	29	1.25	0.09
2.7	Blumlein	present	29	3.7	0.27
2.7	without C_{st}	absent	37	1.6	0.14
2.7	without C_{st}	present	37	3.5	0.27
1.0	direct	absent	57	1.0	0.07
1.0	direct	present	57	0.29	0.02
1.0	Blumlein	absent	29	1.1	0.085
1.0	Blumlein	present	29	1.32	0.105
1.0	without C_{st}	absent	37	0.85	0.067
1.0	without C_{st}	present	57	2.0	0.125

of diameter above 2 cm) was weaker (the output power approximately doubled). Similarly to [12], we investigated the influence of the HBr addition on the properties of the capacitive-discharge-pumped CuBr laser. Our experiments showed that the HBr addition into small-diameter tubes (~ 1 cm) almost did not change the average output power at pump powers below 1 kW, the influence of the HBr addition being mainly manifested in the possibility of operating at higher pump powers (above 1.3 kW). The positive influence of the HBr addition in the case of capacitive-discharge pumping is clearly observed in GDTs with large discharge-channel diameters (Fig. 4). In the GDT of diameter 2.7 cm, the increase in the average output power after the addition of HBr occurs in the entire power range. Nevertheless, a threshold input power also exists (~ 0.9 kW under our experimental conditions) at which the influence of the HBr addition becomes stronger.

Figure 5 presents typical oscillograms for the circuit without an external storage capacitor. Unlike pumping by a glow discharge, the current pulse amplitude almost does not decrease after the addition of HBr, and the current pulse duration also changes insignificantly. At the same time, the current rise time considerably increases at the initial stage of the discharge development (for the first 20 ns). This should lead to the faster voltage growth across the active plasma resistance. As a result, the pumping efficiency increases.

It is also important to point out another peculiarity of the influence of the HBr addition. The addition of HBr to the active medium of a traditionally pumped CuBr laser leads to a considerable increase in the laser pulse duration [12]. In the case of capacitive-discharge pumping, the

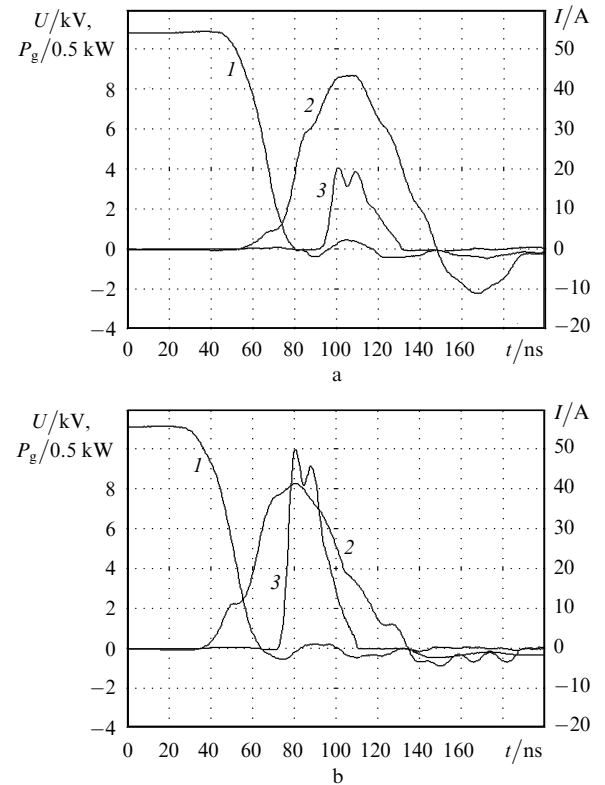


Figure 5. Oscillograms of voltage (1) and pump current (2) pulses and the CuBr laser pulse (3) obtained by using the circuit without the external storage capacitor without the HBr addition ($P_{\text{av}} = 1.4$ W) (a) and with the HBr addition ($P_{\text{av}} = 3.5$ W) (b); $U_{\text{hv}} = 6$ kV.

increase in the pulse energy is mainly achieved due to increasing the peak power by more than two times (Fig. 5). This property can be useful in applications when the employment of short radiation pulses with high peak powers is preferable.

4. Analysis of processes in the discharge circuit of the laser

The voltage across a GDT anode in a circuit without an external storage capacitor is equal to the voltage across a tacitron anode, i.e. across the total GDT resistance, according to the equivalent circuit (Fig. 6a). In circuits with an external storage capacitor, we also measure voltage across the total GDT resistance (Fig. 6b). In both cases, it is impossible to measure voltage directly across the active plasma resistance and electrode capacities. This problem was solved by placing metal (copper) probes in the electrode regions of the GDT, which were placed on the inner wall of the GDT near the active region (Fig. 1). Such an arrangement of the probes allows us to measure in fact the voltage across the internal plates of electrode capacities C_{e1} and C_{e2} . Because the structure of near-electrode layers and, therefore, their capacities and active resistances cannot be determined under experimental conditions, the active plasma resistance R_a is treated as the active resistance of the entire plasma inside the GDT (the equivalent resistance of a plasma column and near-electrode layers). In our opinion, this assumption does not change the essence of processes proceeding in the discharge circuit of the laser. Knowing the voltage across the probes (U_{pr1} and U_{pr2}) and anode (U_{gdt}), we can measure voltages across the rest of the components of the equivalent circuit (Fig. 6):

$$\begin{aligned} U_{C_{e1}} &= U_{gdt} - U_{pr1}, \\ U_{C_{e2}} &= U_{pr2}, \\ U_{R_a} &= \Delta U_{pr} = U_{pr2} - U_{pr1}. \end{aligned} \quad (1)$$

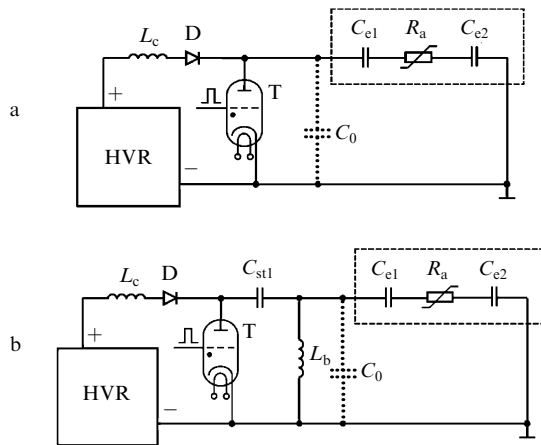


Figure 6. Equivalent circuits of capacitive-discharge pumping of the laser: circuit without the external storage capacitor (a) and the circuit of the directly discharged storage capacitor (b): (HVR) high-voltage rectifier; (C_{st1}) storage capacitor; (L_b) shunting inductance; (L_c and D) charging choke and diode, respectively; (T) tacitron; (C_{e1} and C_{e2}) electrode capacitances; (R_a) active plasma resistance; (C_0) parasitic capacitance.

Figure 7 presents oscillograms of the voltage across the probes and GDT anode, the current through the GDT, and the laser pulse for a circuit without an external storage capacitor, and also the time dependences of U_{R_a} and $U_{C_{e1}}$ calculated by (1). Let us analyse the results obtained when the output voltage of the high-voltage rectified was $U_{hv} = 5.8$ kV. By the instant of switching on the commutator, the electrode capacitor C_{e1} and C_{e2} prove to be charged up to voltages $U_{C_{e1}} = +8$ kV and $U_{C_{e2}} = +2.5$ kV, i.e. $U_{C_{e1}}$ considerably exceeds $U_{C_{e2}}$. In this case, $U_{R_a} = 0$, which is confirmed by the equality of voltages $U_{pr2} = U_{pr1}$ [curves (2) and (3) in Fig. 7]. At the moment of switching on the commutator, the capacitor C_{e1} discharges to the voltage approximately $+2.5$ kV, i.e. $\Delta U_{C_{e1}} \approx 5.5$ kV. At the same time, C_{e2} recharges to the voltage $-2.5 \dots -3$ kV, i.e. $\Delta U_{C_{e2}} \approx 5.5$ kV. Thus, during a period between pulses a negative charge is accumulated in the anode region near the electrode and a positive charge – in the cathode region near the electrode. During a current pulse, the redistribution of the charges occurs and the upper laser levels are simultaneously pumped.

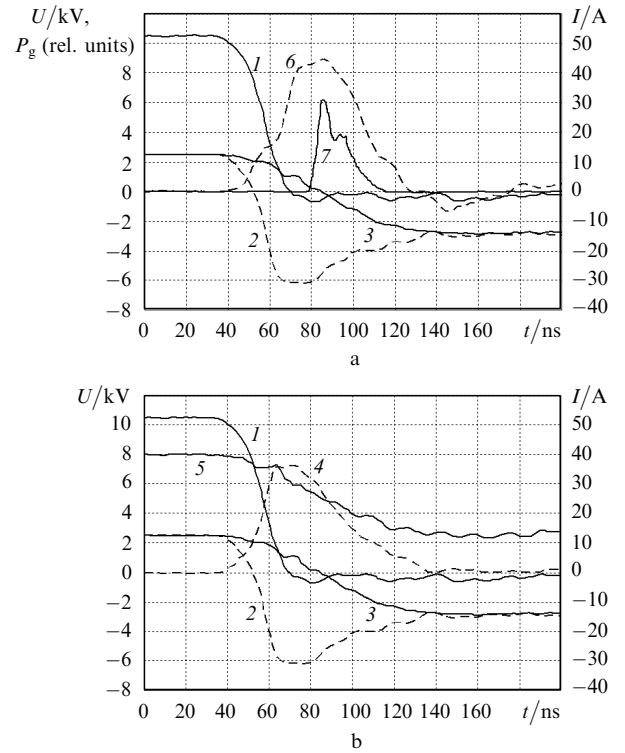


Figure 7. Oscillograms of the basic characteristics of the laser: U_{gdt} (1), U_{pr1} (2), U_{pr2} (3), U_{R_a} (4), $U_{C_{e1}}$ (5), current through the GDT (6) and laser pulse (7). Circuit without the external storage capacitor; $U_{hv} = 5.8$ kV, $f = 37$ kHz, $P_{av} = 1.4$ W.

The oscillograms of the voltage across the probes and GDT anode, of the current through the GDT and laser pulse for the circuit of the direct discharge of a storage capacitor are presented in Fig. 8, where the calculated time dependences of U_{R_a} and $U_{C_{e1}}$ are also shown. By the end of the pulse repetition period, the voltage across electrode capacitors C_{e1} and C_{e2} is zero because the inductance L_b shunts the GDT during the charging of the storage capacitor C_{st1} (Fig. 6b). At the moment of tacitron switching on, the charging of electrode capacitors begins [curves (3) and (5)]

in Fig. 8b) and continues until the equality of voltages $U_{C_{e1}} + U_{C_{e2}} = U_{gdt}$ is achieved. The current flowing through the active medium at this time interval produces the potential difference across the active resistance of the plasma [curve (4) in Fig. 8b], and the upper laser levels are pumped. Thus, lasing occurs during the flow of the charging current of electrode capacitors.

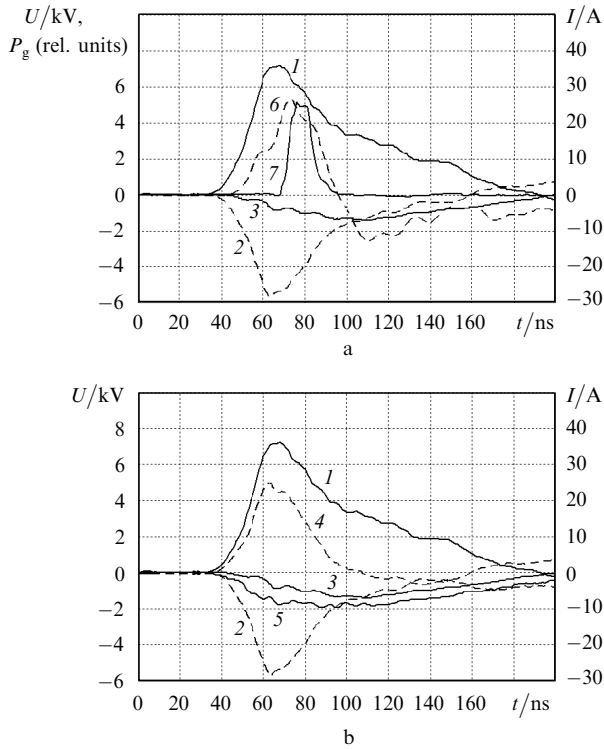


Figure 8. Oscillograms of the basic characteristics of the laser: U_{gdt} (1), U_{pr1} (2); U_{pr2} (3), U_{Ra} (4), $U_{C_{e1}}$ (5), current through the GDT (6) and laser pulse (7). Circuit of the directly discharged storage capacitor; $U_{hv} = 5.8$ kV, $f = 57$ kHz, $P_{av} = 1$ W.

As follows from Figs 7 and 8, the circuit without the external storage capacitor provides the greater discharge current amplitude and, hence, the greater voltage across the plasma compared to the direct circuit for the same consumed power. This provides a more efficient energy supply to the discharge. The presence of a shunting inductance L_b in the direct and Blumlein circuits leads to current oscillations in the period between pulses and voltage oscillations across the probes and active plasma resistance (Fig. 9a). On the one hand, this causes additional energy losses in the discharge circuit, and on the other – the additional population of the metastable states of copper atoms. As a result, when the direct pumping circuit is used, the threshold energy input to the discharge, which is required to compensate for energy losses for excitation of HBr molecules, is not achieved, and, therefore, the addition of HBr reduces the average lasing power for GDTs of diameters 1 and 2 cm (see Table 1).

The oscillatory behaviour of the time dependences of the discharge current and voltage across the GDT during period between pulses, when the direct pumping circuit was used, was pointed out in [6]. Experiments with different shunting inductances showed that the frequency and decay rate of these oscillations are determined by the parameters of the

circuit formed by the GDT and shunting inductance. The shunting inductance in these experiments was varied from 0.03 to 0.3 mH, the average lasing power being virtually invariable. Although the pump current pulse amplitude in the circuit without the external storage capacitor considerably exceeds this amplitude in the direct circuit, the prolonged oscillatory process after the pump pulse is absent in the former case (Fig. 9b). This should reduce the undesirable population of metastable levels during the period between pulses. The reduction of the electron concentration during this period in the circuit without the external storage capacitor also will occur faster than in the direct circuit. The addition of HBr, as upon traditional pumping, improves the electrical matching of the pumping circuit and GDT, which is confirmed by the decrease in the amplitude of the negative current spike after the pump pulse (Fig. 5).

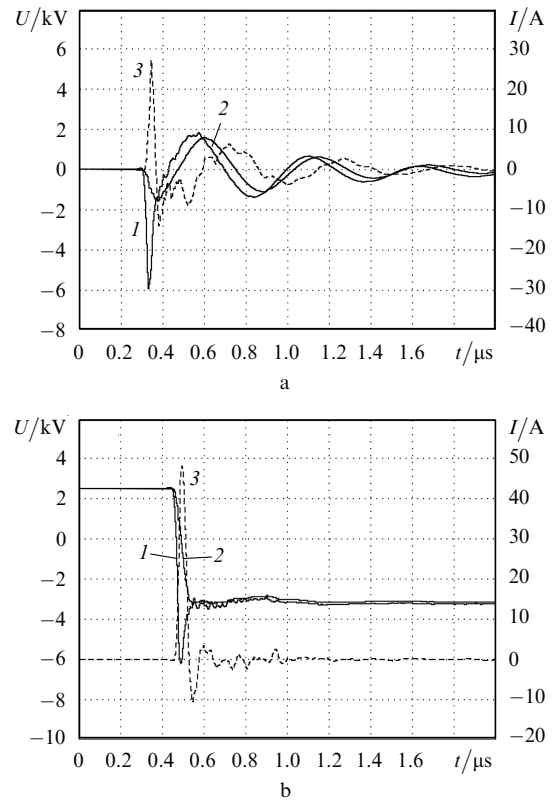


Figure 9. Oscillograms of voltages across probes U_{pr1} (1) and U_{pr2} (2) and current through the GDT (3) for the direct pumping circuit ($U_{hv} = 5.8$ kV, $P_{hv} = 1.1$ kW) (a) and circuit without the external storage capacitor ($U_{hv} = 5.8$ kV, $P_{hv} = 0.9$ kW) (b).

5. Conclusions

The relatively high electrode capacitances in capacitive-discharge-pumped CuBr lasers (comparable with the storage capacitance in the pumping circuit) allow the exclusion of a storage capacitor and a shunting inductance from the circuit. In this case, the GDT self-capacitance, i.e. the equivalent electrode capacitance plays the role of an energy storage system. Our investigations have shown that the circuit without the external storage capacitor is most convenient for pumping external-electrode CuBr lasers.

This circuit is the simplest and its efficiency considerably exceeds the efficiency of the popular circuit of the directly discharged storage capacitor. The circuit without the external storage capacitor also offers an advantage over the Blumlein circuit because it can operate at higher pulse repetition rates.

The addition of HBr into the active medium of capacitive-discharge-pumped CuBr lasers provides the two-fold and higher increase in the average lasing power and efficiency. However, unlike the usual repetitively pulsed high-current discharge with internal electrodes, the maximum effect upon capacitive-discharge pumping is achieved in tubes with large discharge channel diameters. The addition of HBr into GDTs of small diameter does not increase considerably the lasing power in the working range of pump powers. The influence of the HBr addition is revealed only at high pump powers. Another difference is that in the case of capacitive-discharge pumping, the laser pulse energy increases due to the increase in the pulse amplitude rather than its duration, as upon conventional pumping.

The upper laser levels in self-contained capacitive-discharge-pumped metal vapour lasers are excited during the charging of electrode capacitances in circuits with the external storage capacitor and during the discharge of electrode capacitances in the circuit without the external storage capacitor. To excite the laser levels most efficiently upon capacitive-discharge pumping, it is necessary to provide the maximum charging (discharging) rate of electrode capacitances.

Acknowledgements. This work was supported by the Ministry of Education and Science of the Russian Federation (Project No. RNP.2.1.1.5450).

References

1. Batenin V.M., Buchanov V.V., Kazaryan M.A., Klimovskii I.I., Molodykh E.I. *Lazery na samoorganizirovannykh perekhodakh atomov metallov* (Self-contained Metal Atom Lasers) (Moscow: Nauchnaya kniga, 1998).
2. Little C.E. *Metal Vapor Lasers. Physics, Engineering & Applications* (Chichester, UK: John Wiley & Sons Ltd., 1998).
3. Ivanov I.G., Latush E.L., Sem M.F. *Ionnye lazery na parakh metallov* (Metal Ion Vapour Lasers) (Moscow: Energoatomizdat, 1990).
4. Grozeva M., Kocik M., Mentel J., Mizeraczyk J., Petrov T., Telbizov P., Teuner D., Sabotinov N., Schulze J. *Eur. Phys. J. D*, **8**, 277 (2000).
5. Lomaev M.I., Skakun V.S., Tarasenko V.F., et al. *Usp. Fiz. Nauk*, **173**, 201 (2003).
6. Sukhanov V.B., Fedorov V.F., Gubarev F.A., Troitskii V.O., Evtushenko G.S. *Kvantovaya Elektron.*, **37**, 603 (2007) [*Quantum Electron.*, **37**, 603 (2007)].
7. Shiyarov D.V., Evtushenko G.S., Sukhanov V.B., Fedorov V.F. *Kvantovaya Elektron.*, **32**, 680 (2002) [*Quantum Electron.*, **32**, 680 (2002)].
8. Andrienko O.S., Sukhanov V.B., Troitskii O.V., Shestakov D.Yu., Shiyarov D.V. Patent of the Russian Federation, No. 2295811. Priority of 09.11.04.
9. Evtushenko G.S., Petrash G.G., Sukhanov V.B., Fedorov V.F. *Kvantovaya Elektron.*, **28**, 220 (1999) [*Quantum Electron.*, **29**, 775 (1999)].
10. Gubarev F.A., Fedorov V.F., Evtushenko G.S., Sukhanov V.B., Zaikin S.S. *Izv. Tomsk Polytech. Univ.*, **312**, 106 (2008).
11. Shiyarov D.V., Evtushenko G.S., Sukhanov V.B., Bochkov V.D., Kudinov V.N. *Izv. Tomsk Polytech. Univ.*, **307**, 74 (2004).
12. Shiyarov D.V., Sukhanov V.B., Evtushenko G.S., Andrienko O.S. *Kvantovaya Elektron.*, **34**, 625 (2004) [*Quantum Electron.*, **34**, 625 (2004)].